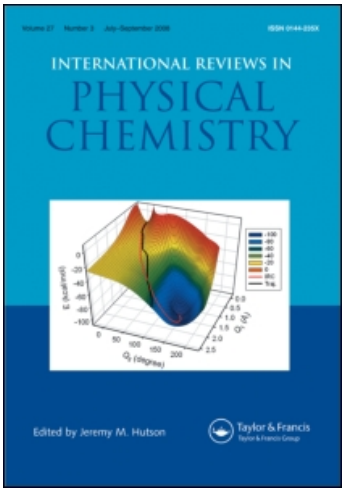

International Reviews in Physical Chemistry
Publication details, including instructions for authors and subscription information:
http://www.informaworld.com/smpp/title~content=t713724383

Manipulating electron wave packets

J. R. R. Verlet; H. H. Fielding

Online publication date: 26 November 2010

To cite this Article Verlet, J. R. R. and Fielding, H. H.(2001) 'Manipulating electron wave packets', International Reviews in Physical Chemistry, 20: 3, 283 — 312
To link to this Article: DOI: 10.1080/01442350117016
URL: http://dx.doi.org/10.1080/01442350117016

INT. REVIEWS IN PHYSICAL CHEMISTRY, 2001, VOL. 20, NO. 3, 283–312

Manipulating electron wave packets

J. R. R. VERLET and H. H. FIELDING†
Department of Chemistry, King's College London, Strand,
London WC2R 2LS, UK

Technological advances over the last decade have led to a significant amount of research being aimed at investigating the time-dependent behaviour of electron wave packets. The ultimate goal is to generate customized wave packets that can control electronic processes in atoms and molecules. Coherent control schemes involving electron wave packets have proved to be of fundamental importance in our quest to understand quantum phenomena. Exotic quantum states such as the Schrödinger cat states have been excited and studied. The wavefunction of a wave packet may now be characterized completely and manipulated into a new form. Autoionization of electron dynamics in complex two-electron systems can be suppressed. Electron wave packets have been excited in molecules. This review provides an overview of the relatively new and rapidly expanding field of electron wave-packet manipulation with particular focus on the experimental achievements and their implications.

Contents

† e-mail: helen.fielding@kcl.ac.uk

International Reviews in Physical Chemistry ISSN 0144–235X print/ISSN 1366–591X online © 2001 Taylor & Francis Ltd
http://www.tandf.co.uk/journals
DOI: 10.1080/01442350110045037

1. Introduction

As early as 1926, it was realized that a spatially localized non-stationary 'classical particle' could be forged from a coherent superposition of quantum-mechanical wavefunctions (Schrödinger 1926). Such superposition states, or wave packets, are particularly fascinating because they allow us to translate exact quantum-mechanical descriptions of atoms and molecules into the more intuitive classical world. Because of technological advances over the last 20 years a significant amount of research is now aimed at studying the time-dependent behaviour of electronic and molecular wave packets with the goal of customizing them to control atoms and molecules.

Several control schemes exist which use light to drive atoms or molecules along predetermined pathways, all of which exploit the coherence of laser light to manipulate the quantum-mechanical phase relationships between the various eigenstates of the system. The frequency domain approach first proposed by Brumer and Shapiro (1986, 1992) and Shapiro and Brumer (1986) is based on the principle that the probability of producing a specified final state from a given initial state depends on the phase relationships between all the independent excitation pathways connecting these states. By employing two coherent light sources with frequencies ω_a and ω_b, which are in resonance with the desired state at energy $a\omega_b = b\omega_a$, and manipulating the relative phases and amplitudes, the population of the desired product may be tuned. A very nice example of this type of control was demonstrated by Zhu *et al.* (1995) who observed modulations in both the H^+ and the HI^+ ion signals due to interference between one- and three-photon excitation paths to photoionizing and photodissociating states of HI. Of more relevance to this review is the time-domain approach first introduced by Tannor and Rice (1985, 1988), which employs sequences of ultrashort light pulses to excite superpositions of molecular eigenstates, or wave packets. The frequencies, amplitudes and phases of the pulses are tailored to steer the wave packet into a predetermined state at a later time. A classic example of this method of control is the experiment of Baumert *et al.* (1991) which uses femtosecond pulses to ionize and dissociatively to ionize the Na_2 molecule. These forms of control have received devoted attention and have been reviewed by several researchers (Tannor and Rice 1988, Brumer and Shapiro 1992, Warren *et al.* 1993, Gorden and Rice 1997). A related approach based on feedback control, developed by Judson and Rabitz (1992), employs iterative computational schemes to custom design optimal laser fields for specific chemical or physical problems. Following the enormous technological advances in pulse tailoring methods, numerous applications to chemical systems have been recorded (Kawashima *et al.* 1995, Weiner 2000). Arbitrary pulses may be generated using devices such as acousto-optic modulators (Hillegas *et al.* 1994) or liquid-crystal modulators (Heritage *et al.* 1985) whose pixels may be programmable, thus creating the desired pulse shape (Weiner *et al.* 1990, Wefers and Nelson 1993). Optimal control theory has been realized experimentally by combining it with learning algorithms in which the laser optimizes its own field with a feedback loop. Bergt *et al.* (1999) recently performed a very elegant experiment exploiting optimal control theory to control organometallic photodissociation branching ratios using feedback-optimized phase-shaped femtosecond laser pulses.

Coherent control and optimal control of molecular dynamics is an extremely active area, but how far can they be applied to electron dynamics? With this review we hope to provide a *coherent* overview of this relatively new field with particular focus on the experimental achievements and their implications.

2. Radial wave-packet dynamics

When a short laser pulse interacts with a hydrogenic atom, a portion of the electron is excited from its ground state to a number of high Rydberg states, creating a Rydberg wave packet. The amplitudes of the individual components of the superposition depend on both the frequency profile of the laser pulse and the square of the dipole moments from the ground state: $\langle nl|er|g\rangle \propto n^{-3/2}$. As a consequence of the electric dipole selection rules, there is negligible contribution from high-angular-momentum states and the wave packet is localized in the radial coordinate only. At short times, the wave packet mimics a classical electron moving on a Kepler orbit. It is created at the inner turning point but subsequently oscillates backwards and forwards between the inner and outer turning points. At longer times, the wave packet spreads and begins to exhibit non-classical behaviour. The first experimental observation of a radial wave packet was only reported just over a decade ago (ten Wolde *et al.* 1988), despite some earlier theoretical work (Alber *et al.* 1986, Parker and Stroud 1986a, b); however, there has since been a great deal of interest in the subject (for example Yeazell *et al.* (1990 1991), Meacher *et al.* (1991), Broers *et al.* (1993), Wals *et al.* (1994), Jones (1996), Lankhuijzen and Noordam (1996), Schumacher *et al.* (1997), Lyons *et al.* (1998) and Ramswell *et al.* (1999)) (see also the excellent reviews by Alber and Zoller (1991) and Jones and Noordam (1997) and references therein).

Radial wave packets are especially attractive as they have some remarkable properties. For example, the spatial extent of a Rydberg state scales as n^2 and so, for a wave packet with average principal quantum number $n = 50$, the inner and outer turning points are over one quarter of a micron apart—almost macroscopic. Of course, under laboratory conditions, there is a limit to how high in the Rydberg series one may excite owing to interactions with the surroundings such as incoherent decay by black body radiation, neighbouring electron–ion complexes or stray fields (Gallagher 1994). Another peculiarity is the period of electronic motion. A wave packet with average $n = 50$ will have a classical orbit period of almost 20 ps, which is of the same order of magnitude as molecular rotation and is more than one thousand times slower than a typical molecular vibration. Consequently, the Born–Oppenheimer approximation breaks down for electron wave-packet states in a molecule.

Because of the vast spatial extent of the Rydberg states involved in these superposition states, the electron wave packet may be considered to spend most of its time sufficiently far away from the core to feel only the Coulombic potential of the positive charge of the ion left behind. It is worth noting that this potential is mathematically identical with the gravitational field felt by a planet orbiting a large star. The distance r_c, beyond which the electron experiences the $1/r$ field is determined by the size of the core. For hydrogen, the electron will always feel such a potential, but when considering other one valence electron systems such as the sodium or potassium atoms which have an electron cloud around the nucleus, the Rydberg electron will feel a Coulomb potential at a distance $r > r_c$ but a more complex potential when it enters the core region and interacts with the remaining core electrons.

Assuming that the radial motion is separable from the angular part, the radial part of the Schrödinger equation may be written as

$$\frac{d^2\psi_\lambda}{dr^2} + \left(2\varepsilon + \frac{2}{r} - \frac{\lambda(\lambda+1)}{r^2}\right)\psi_\lambda = 0, \tag{1}$$

where the term in large parentheses is twice the radial kinetic energy of the electron. This equation has been studied extensively and solutions to it are well documented (Fano 1970). Within the classically allowed limit $\varepsilon < 0$, the solutions of (1) have the form

$$\psi_\lambda(\nu, r) : \left\{ \begin{matrix} f_\lambda(\nu, r) \\ g_\lambda(\nu, r) \end{matrix} \right\}, \tag{2}$$

where

$$\varepsilon = -\frac{1}{2\nu^2}. \tag{3}$$

These two solutions are real oscillatory functions shifted by a phase from each other and are regular and irregular respectively at the origin $r = 0$. For hydrogen, the radial differential equation must be satisfied at all r (including $r = 0$). We can thus say that, since the only regular solution at the origin is $f_\lambda(\nu, r)$, the irregular Coulomb function must be discarded. When the core has a finite size, which is the case for all other atoms and for molecules, the irregular function is also required since the Coulombic potential does not penetrate to $r = 0$ owing to the core electrons. The wavefunction for any atom in a region $r > r_c$ is therefore expressed as a linear combination of the two Coulomb functions:

$$\psi_\lambda(\nu, r) = af_\lambda(\nu, r) + bg_\lambda(\nu, r), \tag{4}$$

where a and b determine contributions of the individual functions and are chosen to be

$$\begin{aligned} a &= \cos(\pi\mu_\lambda), \\ b &= -\sin(\pi\mu_\lambda). \end{aligned} \tag{5}$$

a and b are therefore determined entirely by a constant μ_λ. When $\mu_\lambda = 0$ or 1, the solution is hydrogenic and, when $\mu_\lambda = \frac{1}{2}$, the irregular solution is the sole contributor to the wavefunction.

Of course, these functions need to satisfy certain boundary conditions. In particular, when considering bound states, the wavefunction must vanish as r approaches infinity. The asymptotic form of the Coulomb functions are

$$\psi_\lambda(\nu, r \to \infty) : \left\{ \begin{matrix} f_\lambda(\nu, r \to \infty) \to C(r) \sin[\pi(\nu - \lambda)] \exp\left(\frac{r}{\nu}\right) \\ g_\lambda(\nu, r \to \infty) \to C(r) \cos[\pi(\nu - \lambda)] \exp\left(\frac{r}{\nu}\right) \end{matrix} \right\}, \tag{6}$$

where $C(r)$ is a function that goes to zero more slowly than the exponential blows up as $r \to \infty$. We are now in a position to write the radial wavefunction in the asymptotic limit and impose the boundary condition on it:

$$0 = \psi_\lambda(\nu, r \to \infty) \to \{\sin[\pi(\nu - \lambda)] \cos(\pi\mu_\lambda) + \cos[\pi(\nu - \lambda)] \sin(\pi\mu_\lambda)\} C(r) \exp\left(\frac{r}{\nu}\right). \tag{7}$$

For a bound state, the term inside the curly brackets must equal zero and, as λ is an integer, the boundary condition may be expressed as

$$[\tan(\pi\nu) + \tan(\pi\mu_\lambda)] \equiv \sin[\pi(\nu + \mu_\lambda)] = 0. \tag{8}$$

The second of these identities is only zero when $\nu + \mu_\lambda = n = 0, \pm 1, \pm 2, \ldots$. Not all of these solutions are sensible and values with any physical meaning are those where $n = \lambda + 1, \lambda + 2, \ldots$ and hence $\nu = n - \mu_\lambda$. So we can see that the energy levels n of a particular Rydberg series are shifted by μ_λ with respect to the hydrogenic series. The phase shift $\pi\mu_\lambda$ or quantum defect μ_λ is almost energy independent because the electron kinetic energies are extremely large at the core.

This Coulomb wavefunction approach to the Rydberg problem forms the basis of multichannel quantum defect theory (Seaton 1966, 1983) which is most commonly employed to describe interactions of Rydberg series with ionization or predissociation continua or with other series in both atoms and molecules. A time-dependent extension to this has been proposed (Alber *et al.* 1986) and used to model real atomic (Robicheaux and Hill 1996, Lyons *et al.* 1998, Ramswell and Fielding 1998, Texier and Robicheaux 2000) and molecular (Fielding 1994, 1997, Texier and Jungen 1998, 1999, Texier *et al.* 2000) systems.

A superposition of these Coulombic states, excited from a tightly bound lower state, will evolve along the radial coordinate. The period of motion is $\tau_{\mathrm{cl}} = 2\pi\bar{n}^3$, where $\bar{n}$ is the average principal quantum number in the superposition. However, as already mentioned, the wave packet spreads owing to the anharmonicity of the atomic potential. At longer times the head of the wave packet catches up with the tail and the wave packet is effectively smeared out along the radial coordinate between the classical inner and outer turning points. There is now no longer any analogy with classical mechanics. A series of interference patterns with localized islands of probability distribution are generated at well-determined times. For a wave packet composed of n Rydberg states, $n - m$ ($m = 1, 2, \ldots, n - 1$) miniature wave packets may be observed at times $T_{\mathrm{m}} = T_{\mathrm{rev}}/(n - m)$, where $2T_{\mathrm{rev}} = T_{\mathrm{R}} = 2\bar{n}\tau_{\mathrm{cl}}/3$. T_{R} is the revival time as defined by Averbukh and Perelman (1987). At time $t = T_{\mathrm{m}}$, peaks are observed in the recurrence spectrum at $\tau_{\mathrm{cl}}/(n - m)$ (figure 1). Such partial revivals are a direct consequence of quantum interference and have no classical analogue.

The revivals and fractional revivals can be obtained by expanding the energy E_n around the average energy $E_{\bar{n}}$. A Taylor-series expansion gives the following expression for the energy:

$$\begin{aligned} E_n &= -\frac{1}{2n^2} \\ &= -\frac{1}{2(\bar{n} + \delta n)^2} \\ &= -\frac{1}{2\bar{n}^2}\left[1 - 2\frac{\delta n}{\bar{n}} + 3\left(\frac{\delta n}{\bar{n}}\right)^2 - 4\left(\frac{\delta n}{\bar{n}}\right)^3 + \ldots\right], \end{aligned} \tag{9}$$

where $\delta n = \bar{n} - n$ and $\delta n \ll \bar{n}$. The first term in the square brackets simply yields the average energy of the wave packet. The term linear in δn gives the harmonic energy spacing and yields the classical evolution of the wave packet: $\tau_{\mathrm{cl}} = 2\pi\bar{n}^3$. The quadratic first order anharmonic term gives rise to the revival time. Similarly, higher-order terms (cubic) introduce additional dispersion but materialize slowly (see arrow in figure 1). The cubic term leads to the 'super' revival time (Wals *et al.* 1995).

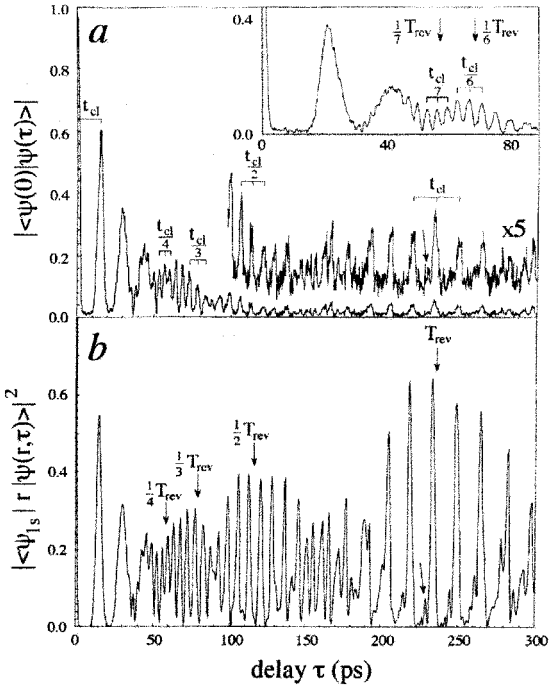

Figure 1. (*a*) Experimental and (*b*) calculated recurrence spectra of a radial wave packet excited at around $\bar{n} = 46.5$ ($\Delta n \approx 6.5$) in rubidium clearly showing a full revival T_{rev} about 237 ps after creation. Second-, third- and fourth-order partial revivals are also visible at the fractional revival times, $T_{rev}/2$, $T_{rev}/3$, and $T_{rev}/4$, respectively. The inset shows even higher-order partial revivals (sixth and seventh order) for a wave packet excited at $\bar{n} = 53.3$, $\Delta n \approx 9.9$. (Figure 1 from Wals *et al.* (1994).)

The long-time dynamics of radial wave packets have been described in detail by Averbukh and Perelman (1989) and also by Alber *et al.* (1986), Parker and Stroud (1986a, b), Gaeta and Stroud (1990) and Wals *et al.* (1995). It was pointed out by Averbukh and Perelman that the miniature wave packets observed in a partial revival have a defined phase relationship between them and they gave an analytical expression for these interference effects. A second-order partial revival may be written as

$$\Psi_2(r,t) = (2)^{-1/2}\left[\exp\left(-\frac{i\pi}{4}\right)\Psi_{cl}(r,t) + \exp\left(\frac{i\pi}{4}\right)\Psi_{cl}(r,t+\tfrac{1}{2}\tau_{cl})\right]. \qquad (10)$$

The two partial wave packets have a $\pi/2$ phase difference between them and similar results can be obtained for higher-order partial revivals. This phase difference can be exploited to engineer some remarkable quantum states which will be discussed in detail below.

3. Dynamics of interfering wave packets

Before the interference of more than one wave packet in a Rydberg system was used to generate unique quantum states, it was employed as a detection method.

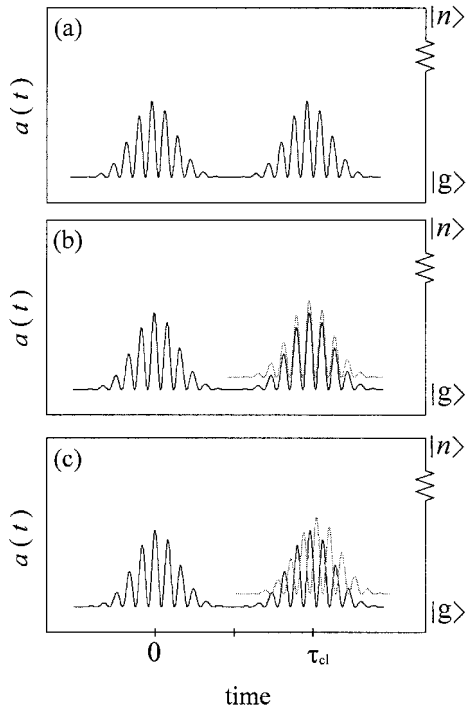

Figure 2. (*a*) Rabi oscillations in the population amplitudes of Rydberg states $|n\rangle$ excited at a time $t = 0$ from a ground state $|g\rangle$ using a single short laser pulse. Away from the core, the electron is decoupled from the molecular ion until it returns after a full orbit, τ_{cl}. After time τ_{cl}, a second identical short laser pulse interacts with the atom (.....) and, depending on the phase difference between the two pulses, the Rabi oscillation amplitudes are (*b*) doubled if they are in phase and they interfere constructively or (*c*) zero when out of phase and and they interfere destructively.

3.1. *Optical Ramsey method*

The idea of exciting a second wave packet in a Rydberg system, using an identical but delayed laser pulse, to monitor the evolution of the first wave packet was first suggested by Noordam *et al.* (1992). The technique was adapted from a similar scheme that had been developed for molecular wave packets (Scherer *et al.* 1990, 1991). The technique is explained properly later in this section using perturbation theory but it is useful to acquire a physical picture first.

With reference to figure 2, the ground state $|g\rangle$ will couple to a number of Rydberg states upon irradiation with a picosecond pulse. This coupling manifests itself as Rabi oscillations at the optical frequency, defining the time-dependent population amplitude $a_n(t)$ of the Rydberg states $|n\rangle$. When a second identical but delayed phase-coherent probe wave packet is excited, it too will couple the Rydberg states with the ground state in a similar fashion. However, whenever the pump wave packet is localized at the core (at a multiple of the orbit period for short times), the second probe wave packet will oscillate between being in phase or out of phase with the first pump wave packet, depending on the relative phases of the excitation pulses. When in phase, the oscillation in $a_n(t)$ is doubled and the Rydberg population is $|2a_n(t)|^2$. When out of phase, the Rydberg population is pumped back down to the ground state. As the first pump wave packet moves away from the core region, the

Rydberg electron is decoupled from the core and the probe wave packet will simply undergo Rabi oscillations independently, such that the total Rydberg population is the statistical (incoherent) sum $2|a_n(t)|^2$. The population may be monitored with almost unit efficiency using a delayed pulsed electric field to ionize the Rydberg states. This has an obvious advantage over earlier pump–probe experiments using photoionization which suffers from low absorption cross-sections and a comparatively pitiful signal-to-noise ratio. Experimentally, this scheme requires precise control of the phase difference between the two optical pulses, which in turn requires a stabilized interferometer. This may be accomplished by locking a feedback circuit on to a fringe pattern generated in the same interferometer, an example of which has been discussed in detail by Hong *et al.* (1998).

3.2. *Young's double-slit experiment*

Young's double-slit experiment is fundamental to wave mechanics and is central in fields such as coherence and optics. Although the optical Ramsey method itself has been described as a temporal analogue of Young's double-slit experiment (Metiu and Engel 1990), Noel and Stroud (1995) have reported a beautiful atomic analogue of the double-slit experiment in which interference patterns generated by two overlapping wave packets are monitored by a third wave packet.

In Young's original experiment, a light source was shone at an opaque screen containing two slits, resulting in two coherent sources of light. An interference pattern of fringes was then observed on a screen in the distance where the beams overlapped spatially. In the atomic analogue, two wave packets are excited at different ends of the radial coordinate representing the two coherent light sources. These wave packets are then allowed to propagate and interfere and the interference pattern is monitored using a third wave packet as the probe.

The Noel–Stroud experiment employed picosecond laser pulses to generate radial wave packets in an atomic beam of potassium. The average principal quantum number of the superpositions was approximately $\bar{n} = 66$. Two identical wave packets were excited with a delay of half the Kepler orbit period plus a controlled phase shift ϕ between them. In order to observe any interference between the two wave packets they must overlap spatially and so they were allowed to evolve to the second-order partial revival. The resulting interference pattern was then monitored by the optical Ramsey method using a third pulse identical with the first two (figure 3). When the phase difference between the two pump pulses is $\phi = \pi/2$, the wave packets interfere in such a way that they interfere constructively at the outer turning point, enhancing the radial probability density, and destructively at the inner turning point, depleting the radial probability density. On the other hand, when $\phi = -\pi/2$, the situation is reversed and the radial probability density is at the inner turning point. In both of these examples with pairs of wave packets with $\phi = \pm\pi/2$ phase difference, the interference pattern is that of a full revival with the electron density passing through the core region at multiples of the classical orbit period. However, the Ramsey fringes are π out of phase with one another, which results in the region of constructive interference occurring at opposite ends of the radial coordinate for the two cases. A third, perhaps more interesting situation arises when the phase shift is set to $\phi = \pi$. The wave packets at their partial revivals interact in such a way that an electron density remains at both the inner and outer turning points, creating a quantum state which never comes to a full revival but is 'stuck' in the second order partial revival. Such a state cannot be generated by single-photon excitation and is

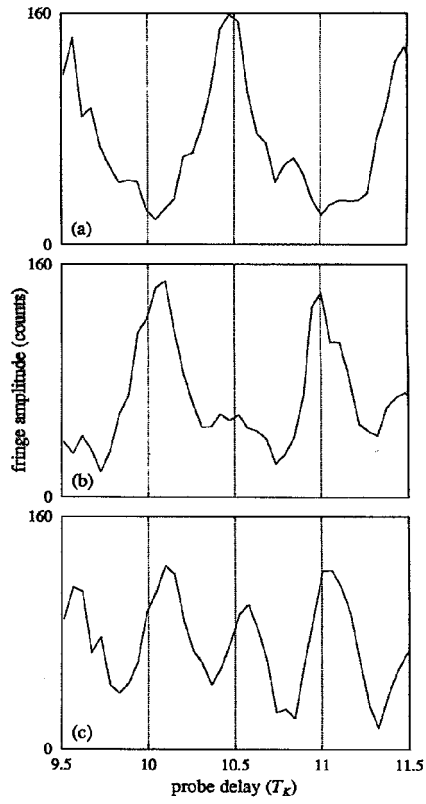

Figure 3. A plot of the amplitude of Ramsey fringes generated by a pair of interfering wave packets at the second order partial revival (around 10 ps) as obtained by Noel and Stroud (1995, figure 4). The two wave packets are excited with a delay of half an orbit period between them plus a controlled phase difference. The phase determines the nature of the interference: (*a*) $\pi/2$, the resultant wave packet is localized at the outer turning point; (*b*) $-\pi/2$, the wave packet is localized at the inner turning point; (*c*) π, the wave packet is localized at both the inner and the outer turning points creating a quantum state which is 'stuck' in a second order partial revival. (Figure 4 from Noel and Stroud (1995).)

an atomic representation of the Schrödinger cat state which is discussed in more detail later in this section.

These interference patterns can be explained in a visual way using the cartoon plots of figure 4. At a second-order partial revival, the portion of the wave packet at the outer turning point is phase shifted by $\phi = \pi/2$ with respect to the portion at the inner turning point. This is depicted in figure 4 (1). Adding a second wave packet, (figure 4 (2a)) with a delay of half the Kepler orbit and no phase shift, $\frac{1}{2}\tau_{cl} + \phi$ (where $\phi = 0$), the two wave packets (figure 4 (1) and figure 4 (2a)) interfere in such away that there are still portions of wave packet at each turning point (figure 4 (3a)). Introducing a phase shift of $\phi = \pi/2$ in the second wave packet (figure 4 (2b)) whose relative phases in the second-order partial revival are π and $\pi/2$ at the inner and outer turning points respectively results in destructive interference at the inner turning point because these two portions of wave packet are π out of phase. The interference is constructive at the outer turning point where they are in phase (figure

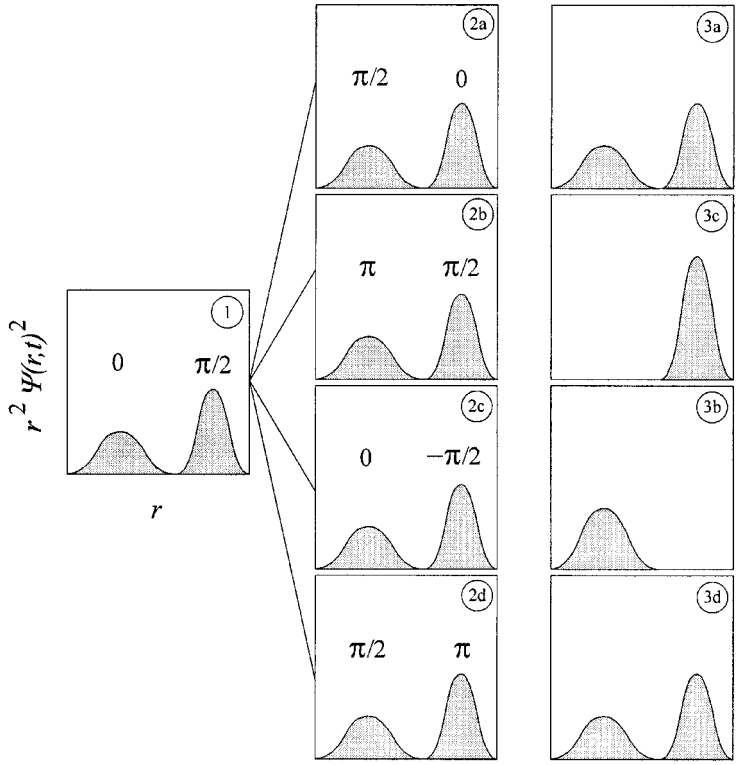

Figure 4. The dynamics of interfering wave packets can be visualized using these simple cartoon plots. In this example, two wave packets are allowed to interfere at their second-order partial revival, according to the experiments performed by Noel and Stroud (1995). (1) shows the first wave packet at its partial revival with the relative phases of the two 'little wave packets'. (2a) shows the second wave packet, which is excited half an orbit period later, at its partial revival, with the phases of the two components relative to those of wave packet (1). Wave packets (1) and (2a) are allowed to interfere and the resulting electron density as a function of radial distance r, is illustrated in (3a). (2b), (2c) and (2d) show the second wave packet with its relative phases when controlled phase shifts of $\phi = \pi/2, -\pi/2$ and π respectively have been added. (3b), (3c) and (3d) show the resultant electron density when wave packet (1) interacts with wave packets (2b), (2c) and (2d) respectively.

4 (3b)). Similarly, figure 4 (3c) shows the interference of the first wave packet with a second having a phase shift of $\phi = -\pi/2$ (figure 4 (2c)), and figure 4 (2d) and figure 4 (3d) explain the pattern for $\phi = \pi$.

3.3. *Excitation of Schrödinger's 'live' and 'dead' cat*

Noel and Stroud (1996) have also excited an atomic state resembling Schrödinger's paradoxical cat which highlights the difficulty in drawing the quantal–classical boundary. A cat placed in a box with a deadly source of poison is described as a superposition of both a 'dead' cat and a 'live' cat. Classically, however, the cat must obviously be either dead or alive. Only upon opening the box (observation) will the cat be in one distinct state or the other.

A Schrödinger cat state is formed from a superposition of two classical states which are macroscopically distinguishable. In an atom, a classical state exists in a

harmonic potential. Although an atomic potential is only approximately harmonic, the electronic wave packet retains classical behaviour for several orbit periods before the wave packet disperses. At short times, the potential may be treated as a parabolic potential, and the problem may be described by the Hermite equation. Its eigenfunctions have a definite parity and are called either even or odd states, $|\alpha\rangle + |-\alpha\rangle$ and $|\alpha\rangle - |-\alpha\rangle$ respectively.

If we now recall the atomic double-slit experiment, two wave packets were excited at either end of the Kepler orbit: one wave packet at the inner turning point and a second wave packet half an orbit period later at the outer turning point. For $\bar{n} = 66$, these wave packets are separated by approximately 0.2 μm. Although this is not quite macroscopic but mesoscopic, the analogy remains significant. The size is restricted by interactions with the surrounding environment in which the Rydberg atom exists and cannot be easily overcome in a laboratory. The atomic cat state can be fully characterized both by using the optical Ramsey method, showing interference in phase space and by state selective field ionization (SSFI) (Gallagher *et al.* 1977). As a consequence of the second wave packet, the state distribution is altered with respect to the single-wave-packet excitation. Two extreme scenarios occur (figure 5). When the phase of the second wave packet is set to zero, the even Rydberg

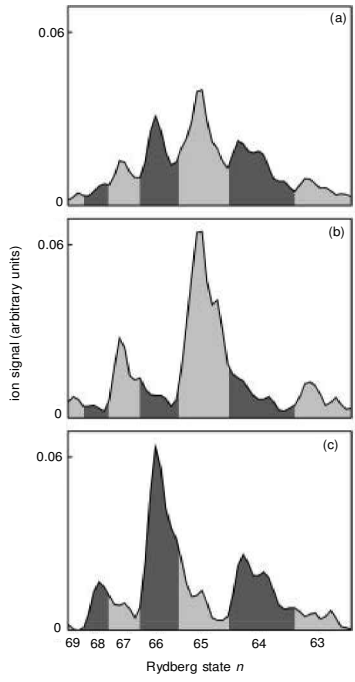

Figure 5. Rydberg state populations of radial wave packets measured using SSFI. The odd Rydberg states are shaded light grey and the even states are shaded black. (*a*) The distribution of a wave packet excited with $\bar{n} = 66$ using a single short pulse. (*b*) The distribution following excitation with a pair of pulses with phase difference π shows that only the odd states survive, analogous to Schrödinger's 'dead' cat. (*c*) The distribution following excitation with a pair of pulses with phase difference 0 shows that only the even states survive, analogous to Schrödinger's 'live' cat. (Figure 1 from Noel and Stroud (1996).)

states are eliminated and only odd Rydberg states are in the superposition. This is analogous to the odd-harmonic-oscillator cat state or, alternatively, the 'dead' cat. 'Live' or even-harmonic-oscillator cat states are excited by imposing a $\phi = \pi$ phase shift, in which only even states survive. Note that these states correspond to those in figure 4, which are in a permanent (neglecting incoherent decay) second-order partial revival state. A simple analysis of this state-selective population using multiple pulses is presented below. These experiments are not restricted to only two phase-coherent wave packets but may be extended to a train of N pulses (Chen and Yeazell 1997a, 1999a, Noel and Stroud 1997) so that an arbitrary wavefunction may be excited.

3.4. *Dynamics of interfering wave packets*

A wave packet formed from a superposition of Rydberg states $|n\rangle$ may be expressed as

$$\Psi(r, t) = \sum_n a_n \psi_n(r) \exp(-\mathrm{i}\omega_n t), \tag{11}$$

where a_n and ω_n are the amplitudes and the eigenenergies respectively of the Rydberg state $|n\rangle$. Applying the rotating-wave approximation which predicts that only the terms involving $\Delta_n = \omega_n - \omega_g - \omega_L$, where ω_g is the ground-state energy and ω_L the laser frequency, will contribute significantly allows us to obtain equations for the population amplitudes. Anticipating that the excitation will be sufficiently weak so that the weak-field limit is valid, the ground-state population amplitude remains unchanged and it is only necessary to consider the rate of change in the Rydberg population:

$$\dot{a}_n = -\frac{\mathrm{i}}{2}\Omega_n a_g f(t) \exp(\mathrm{i}\Delta_n t), \tag{12}$$

where Ω_n is the Rabi frequency of the transition between the initial state and a given Rydberg state. $f(t)$ represent the field to which the system is subjected. In this case, we consider a number N of pulses. If the pulses are assumed to be Gaussian with optical frequency ω_L, the multipulse perturbative field may be written as

$$f(t) = (2\pi\sigma^2)^{-1}\left[\exp\left(-\frac{t^2}{2\sigma^2}\right) + \sum_i^{N-1} \exp\left(-\frac{(t-\tau_i)^2}{2\sigma^2}\right)\exp(\mathrm{i}\omega_L\tau_i)\right], \tag{13}$$

where the sum goes over pulses i, delayed by τ_i with respect to the first pulse. As intended, in the weak-field limit, perturbation theory may be used to derive an expression for the amplitudes of the states in the superposition. In this case, the amplitudes depend directly on the Fourier transform $G(\Delta_n)$ of the excitation field. Note that we have introduced the detuning into the pulse following the rotating-wave approximation:

$$a_n = -\frac{\mathrm{i}}{2}\Omega_n \exp\left(-\frac{\Delta_n^2\sigma^2}{2}\right)\left(1 + \sum_i \exp[i(\Delta_n + \omega_L)\tau_i]\right). \tag{14}$$

A similar result was obtained by Noordam *et al.* (1992) in their proposal of the Ramsey fringe method and by Chen and Yeazell (1997a) who generalized the scheme for any number of pulses. Extending these arguments (Krause *et al.* 1997, Chen and Yeazell 1998b), a similar scheme can be obtained to excite arbitrary wave packets

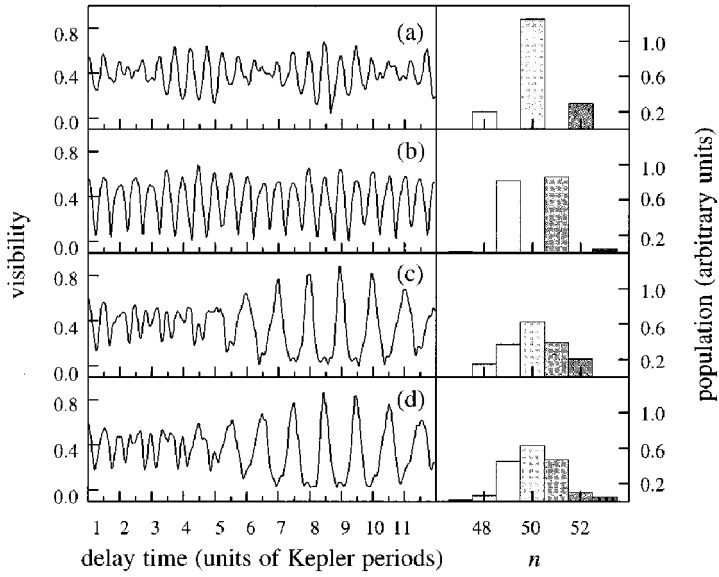

Figure 6. Calculated plots of the amplitudes of the Ramsey fringes and the population distributions following excitation of a pair of interfering wave packets. The first wave packet is allowed to evolve to the outer turning point before the second wave packet is excited and the dynamics and populations of the resultant are probed by a third wave packet. The relative phases of the pulse pair are: (*a*) $\phi = 0$, (*b*) $\phi = \pi$, (*c*) $\phi = \pi/2$ and (*d*) $\phi = -\pi/2$. (Figure 1 from Chen and Yeazell (1997a).)

using optimal control in which the multipulse excitation field is replaced with a single shaped pulse (Schumacher *et al.* 1995).

This expression was used to calculate Rydberg populations following irradiation by multiple pulses and is in very good agreement with the two pulse experiments described above and three pulse experiments implemented by Noel and Stroud (1997).

A particularly appealing form of equation (14) has been given by Chen and Yeazell (1997a) for the two pulse case in which the first pulse is allowed to evolve to the outer turning point before the next wave packet is excited: $\tau_1 = \pi\bar{n}^3$. Having followed their original notation, the frequency terms in the exponent under the sum are replaced by $\Delta_n + \omega_L = \Delta + \omega_n + \omega_{\bar{n}}$, where $\Delta = \omega_n - \omega_g$ is the energy of the centre of the wave packet above the ground state. The eigenfrequency of state $|n\rangle$ may now be expanded according to equation (9) to the first order and substituted in the expression for the amplitudes:

$$a_n = -\frac{\mathrm{i}}{2}\Omega_n \exp\left(-\frac{\Delta_n^2\sigma^2}{2}\right)(1 + \exp\{\mathrm{i}[\phi + (n - \bar{n})\pi]\}), \tag{15}$$

where the phase $\phi = \Delta\tau_1$ determines the outcome of the excitation. The amplitudes a_n of the Rydberg states will only be non-zero if $\phi + (n - \bar{n})\pi$ is an even multiple of π. When $\phi = 0$, this criterion is only obeyed if $n - \bar{n}$ is even. Depending on $\bar{n}$, only even or odd states will be excited in the multipulse excitation. This scenario is identical with the Schrödinger live and dead cats and is shown in figure 6.

3.5. *Reconstruction of a wave packet*

Following detailed theoretical investigation of these shaped wave packets by excitation with multiple optical pulses or tailored pulses, it seemed possible to reconstruct an arbitrary wave packet. The problem of measurement in quantum mechanics is appreciated (Pauli 1933). All information of a quantum state is incorporated in its wavefunction or density matrix. Because these are not experimentally observable, detailed knowledge of the wavefunction is not available. However, there has been theoretical motivation to reconstruct quantum states (Vogel and Risken 1989).

The method for reconstructing an atomic wave packet proposed by Chen and Yeazell (1997b) makes use of a combination of the optical Ramsey method and SSFI, or another high-resolution detection technique. Using SSFI, the population of the constituent Rydberg states as given by $|a_n|^2$ are measured with very high efficiency. These populations determine the population amplitudes except for the common phase factor for the Rydberg states: $a_n = |a_n| \exp(\mathrm{i}\delta_n)$. This phase information may be recovered by cross-correlation of the target wave packet with a well-characterized probe wave packet. By varying the phase between the optical excitation pulses and therefore between the wave packets, by SSFI, the phase information of the initial wave packet may be recovered (Chen and Yeazell 1997b, Weinacht *et al.* 1998a). The use of cross-correlation is the basic method applied in spectral interferometry and has successfully been employed for shaped atomic wave packets by Weinacht *et al.* (1998a). This technique may also be extended to the strong-field limit in which the excitation field is no longer perturbative (Chen and Yeazell 1999b). An alternative approach for determining the complex amplitude has been used by Jones and Campbell (2000) in which the desired phases are retrieved from a time-dependent probability (Jones 1998) and momentum space distribution (Campbell *et al.* 1998).

An optically tailored pulse excites a target wave packet composed of Rydberg states $|n\rangle$:

$$\Psi(t=0) = \sum_n a_n |n\rangle. \tag{16}$$

The wave packet may be shaped using a programmable pulse shaper to shape the optical pulse (Weiner 2000). In the reconstruction experiment by Weinachet *et al.*, a Bragg deflector was used (Tull *et al.* 1996). A second well-characterized optical pulse then excites a second reference wave packet at a controlled time delay:

$$\Psi_{\mathrm{R}}(t=\tau) = \sum_n b_n |n\rangle \exp(\mathrm{i}\omega_g \tau), \tag{17}$$

where $\omega_g \tau$ is the phase acquired by the ground or intermediate state $|g\rangle$, and the resulting wave packet of both target and reference wave packet may be written as

$$\Psi_{\mathrm{T}}(t=\tau) = \sum_n [a_n \exp(-\mathrm{i}\omega_n \tau) + b_n \exp(\mathrm{i}\omega_g \tau)]|n\rangle \tag{18}$$

and the total measured population of a Rydberg state is the cross-correlation of the two wave packets:

$$|\Psi_{\mathrm{T}}|^2 = |a_n|^2 + |b_n|^2 + 2|a_n||b_n| \cos[(\omega_n - \omega_g)\tau - \delta_n]. \tag{19}$$

Being independently tailored, the programmable target pulse is no longer phase locked with respect to the probe pulse and the coherence is lost as the time average of the cosine term tends to zero. However, the relative phase $\delta_{nm} = \delta_n - \delta_m$ may be recovered (Weinacht *et al.* 1998a) by writing the correlation function as

$$r_{nm} = \frac{\langle P_n P_m \rangle - \langle P_n \rangle \langle P_m \rangle}{\Delta P_n \, \Delta P_m} = \cos\left[(\omega_n - \omega_m)\tau - \delta_{nm}\right], \tag{20}$$

where ΔP_n is the standard deviation in P_n. It is now straightforward to extract the desired phase of the population amplitude with respect to a chosen Rydberg state: $\delta_{nm} = \delta_n - \delta_m$. A graphical representation of an arbitrarily chosen wave packet can be found in the paper by Weinacht *et al.*

This technique may be extended in a Rabitz-like feedback loop to create any desired wave-packet wavefunction and may be likened to a form of quantum holography (Weinacht *et al.* 1999). Having reconstructed the wave packet wavefunction, the difference between any desired wavefunction and the measured wavefunction for each Rydberg state component may be calculated. This may then be used to reprogram the pulse shaper and thus the pulse shape in order to alter the phases and amplitudes of the states in the superposition. Running the feedback loop through a few iterations, the desired wave packet is constructed to remarkable precision. This is such a powerful tool since it has the capability of generating designer wave packets which will allow us to manipulate atomic and molecular processes at a very fundamental level.

Recently, Rella *et al.* (2000) measured the phase of a wave packet in a static electric field at the saddle point as the electron was ejected from the atomic potential. Upon ejection of the wave packets, the properties remain unchanged as they are accelerated in the field. At a distance, the electron flux may then be measured. Each of these ejected wave packets will have a relative phase associated with it (Texier and Robicheaux 2000). Using a phase-locked reference pulse, the ionization probability may be controlled. This probability of ejection is determined by the optical phase between the excitation pulses, which defines the coherent sum of the target and reference states. The electron flux is measured using the atomic streak camera (Lankhuijzen and Noordam 1996). In essence, this method is identical with that described earlier; however, the wave-packet characteristics are determined at the saddle point of an atomic potential rather than near the core.

4. The wave packet in three dimensions

So far, this review has focused on the dynamics of radial electron wave packets in hydrogenic systems. Such radial wave packets are generally the most appealing because of their close link with classical dynamics and the ease with which they may be created. Despite the inherent correspondence with a classical electron, a radial wave packet is not a totally correct analogue. There are two reasons for this: a radial wave packet undergoes dispersion owing to the anharmonicity of the atomic potential, and a radial wave packet, as its name implies, is not localized in the angular coordinate. Both of these problems may be overcome by generating a new type of wave packet referred to as a Trojan wave packet. Such a wave packet oscillates along stable points in an atom–rotating field system, closely related to the stable Lagrange points L_4 and L_5 in the Sun–Jupiter restricted three-body problem found in celestial mechanics (Bialynicki-Birula *et al.* 1994). In this problem, a cluster

of asteroids (called the Trojans) oscillates at these stable points in space. The problem may be treated as a *restricted* three-body problem as the mass of the asteroids is significantly smaller than the masses of the two primary bodies and its gravitational field may be ignored. In the atomic analogue, the two primary bodies are replaced by the atomic ion in a circularly polarized laser field and the asteroids are replaced by the electron wave packet which is localized at the stable points of the system. Despite the fact that it is rather difficult to excite such a wave packet, it does present an extraordinary quantum state. This atomic analogue of the Trojan asteroid problem has recently been reviewed by Uzer *et al.* (2000) and the reader is referred to this article. Because of the experimental focus of this review, we shall dwell no further on the Trojan states.

Generation of a wave packet localized in all coordinates in a pure atomic potential has become possible (Bensky *et al.* 1998, Bromage and Stroud 1999) because of the recent development of half-cycle pulses (HCPs) for the excitation and detection of electron wave packets. HCPs are short pulses of electromagnetic radiation but differ from ordinary pulses in that, as their name suggests, they do not undergo full 2π cycles. A HCP is really just an electric field that is rapidly switched on and then off again. The pulse propagates like an electromagnetic wave with a very special property, namely that its time integral is not zero, as it is for ordinary electromagnetic radiation, but has a well-defined value F_{HCP}. The consequence of this non-zero time integral of the electric field is that a HCP can impart momentum to an electron. If the momentum increases sufficiently, bound electrons can escape from the atom and ionize and, contrary to traditional methods, the electron need not be near the core. In fact, a free electron will be influenced by HCPs in much the same way as a bound electron. This feature makes it a significantly more versatile type of radiation than ordinary optical pulses, which restrict detection of the electron to near the core because of the requirement of a nearby massive object to conserve momentum.

For a sufficiently short HCP, such that the electron may be considered to be stationary over the duration of the field, the momentum transferred to the electron may be treated as impulsive. The electron will receive a momentum impulse or 'kick'

$$\mathbf{I} = \int e\mathbf{F}_{\mathrm{HCP}}(t)\,\mathrm{d}t, \tag{21}$$

and the momentum of the electron after this kick is given as

$$\mathbf{p} = \mathbf{p}_0 + \int e\mathbf{F}_{\mathrm{HCP}}(t)\,\mathrm{d}t, \tag{22}$$

where $\mathbf{p}_0$ is the initial momentum of the electron. This sudden change in momentum is accompanied by a change in the energy of the electron:

$$\Delta E = \frac{\mathbf{p}^2}{2m} - \frac{\mathbf{p}_0^2}{2m} = \frac{1}{2m}(\mathbf{I}^2 + 2\mathbf{p}_0 \cdot \mathbf{I}). \tag{23}$$

The energy kick depends only on the initial momentum of the electron and the strength of the electric field.

HCPs have had a considerable impact on studies of stationary states and, although they have been employed widely to ionize Rydberg states and wave packets (Jones *et al.* 1993, Reinhold *et al.* 1993, Tielking and Jones 1995), they have also been used to create Rydberg wave packets (Jones 1996, Reinhold and Burgdörfer 1996,

Raman *et al.* 1996, 1997, Campbell *et al.* 1999). HCPs have also been used to map out the probability distribution of a wave packet in momentum space (Jones 1996).

HCPs are commonly produced in a thin GaAs semiconductor wafer to which a field of less than $10\,\mathrm{kV\,cm^{-1}}$ is applied parallel to the surface. A 100 fs laser pulse induces a coherent electromagnetic pulse to be transmitted through the wafer. This electromagnetic shock wave may then be directed into free space through the side of the dielectric. This HCP has a pulse width of $\tau_{\mathrm{HCP}} \approx 0.5$ ps and a bandwidth of about 1 THz or $33\,\mathrm{cm^{-1}}$ (Morou *et al.* 1981, Auston *et al.* 1984, De Fonzo *et al.* 1987, Fattinger and Grischkowsky 1988, 1989).

Having defined HCPs and described briefly how they are made, it is now possible to move on to describe their implementation in the excitation of three-dimensional wave packets. Gaeta *et al.* (1994) proposed a scheme for the experimental excitation and observation of a spatially localized wave packet involving two distinct steps. The first step involves exciting an eigenstate with chosen eccentricity, such as a circular state (Molander *et al.* 1986, Hulet and Kleppner 1983, Delande and Gay 1988, Chen *et al.* 1993), of an n manifold of an atom subjected to an external low-frequency field. In the second step, a suitable HCP coherently redistributes population into states with the same eccentricity in different n manifolds, forming a wave packet on a defined Kepler orbit. The initial step involves excitation to the chosen n manifold using a nanosecond dye laser. A dc Stark field, sufficiently low that it does not upset the Inglis–Teller limit, is used to lift the degeneracy of the manifold. In one experimental realization of this scheme, Bromage and Stroud (1999) excited the red Stark state in the $n = 30$ manifold of sodium. This 'red' Stark state is the lowest energy state in the manifold and has maximum eccentricity. The probability distribution of this state lies along a line confined to the negative side of the atom with respect to the dc Stark field vector. This excitation technique is equally applicable for a circular state (the state in the middle of the manifold) or a state with any chosen eccentricity.

With the atom excited to the red Stark state of the manifold, a suitable HCP (1 kV peak field; 400 fs full width at half-maximum (FWHM)) coherently redistributes the population into red states of neighbouring n manifolds. HCP momentum transfer processes are conveniently illustrated (figure 7) when one represents the quantum-mechanical probability distribution as an ensemble of classical charges travelling with the same angular speed spread along the orbit. The HCP will induce a momentum kick in each member of the ensemble, depending on their orientation with respect to the HCP field. For a short HCP, this means that the ensemble will now have an energy distribution while remaining in approximately the same positions in coordinate space. The distribution in momentum of the ensemble will cause the low-energy members to catch the high-energy members, leading to a localized population distribution in three dimensions. Redistribution of population into other Stark states of neighbouring manifolds is not favoured as the dipole moments connecting these are significantly lower.

Once the HCP excitation is complete and the wave packet is localized, it will oscillate along a line between the inner turning point and outer turning point. The wave packet may be detected by applying a second strong probe HCP. This probe will give the wave packet a hard kick to ionize it. The dynamics of the wave packet, shown in figure 8, reveal the expected classical oscillations between the turning points. The localized wave packet shows the expected increased ionization at the core as the electronic momentum is greater. This method (Gaeta *et al.* 1994) can be used

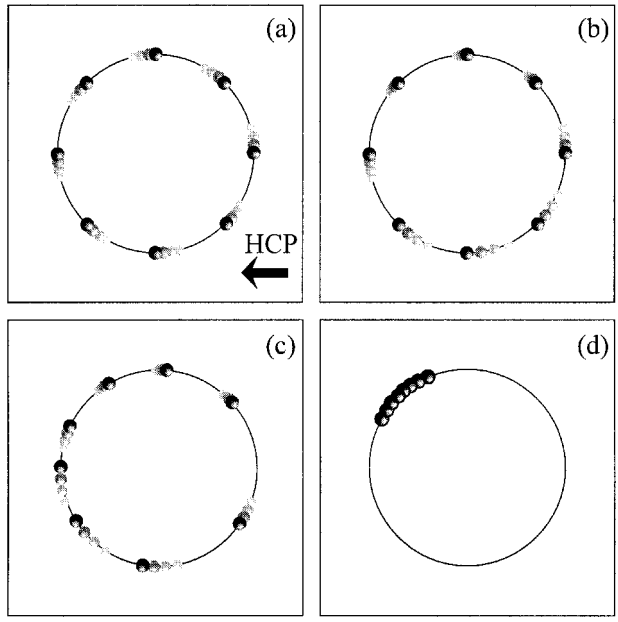

Figure 7. The probability distribution of an electron excited in a circular Rydberg state may be visualized (in two dimensions) by an ensemble of classical particles moving with the same angular velocity on a circle. (*a*) The Rydberg state is subjected to a short HCP which delivers a momentum kick to each member in the direction of the pulse. (*b*) After interaction with the HCP, the members of the ensemble will possess different angular velocities. (*c*) The distribution of the members of the ensemble will become lopsided. (*d*) After some time the members of the ensemble will be localized in one small area of the orbit, forming a wave packet. This is not restricted to circular Rydberg states and any desired eccentricity may be chosen.

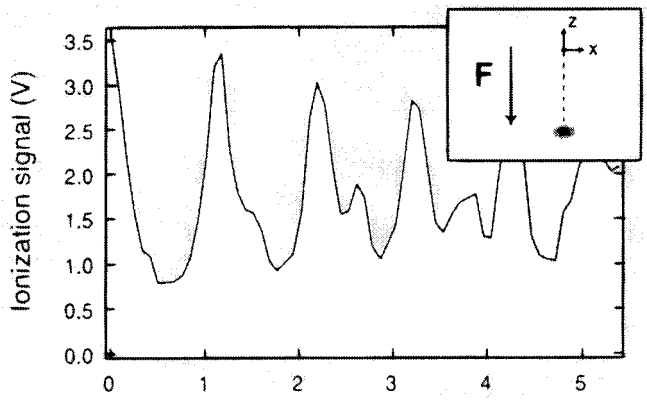

Figure 8. Ionization of a wave packet localized on a linear orbit. The peaks in the signal representing enhanced ionization which occurs when the electron wave packet is at the core since this is where the electron momentum is greatest. The time delay is in units of the 4.1 ps classical orbit period of this particular wave packet. The inset shows the wave packet at its outer turning point and the relative orientation of the kick **F** that it receives from the ionizing HCP pulse. Note that in this example the pulse is kicking the wave packet away from the core so the modulations are very deep and clear. (Figure 3 from Bromage and Stroud (1999).)

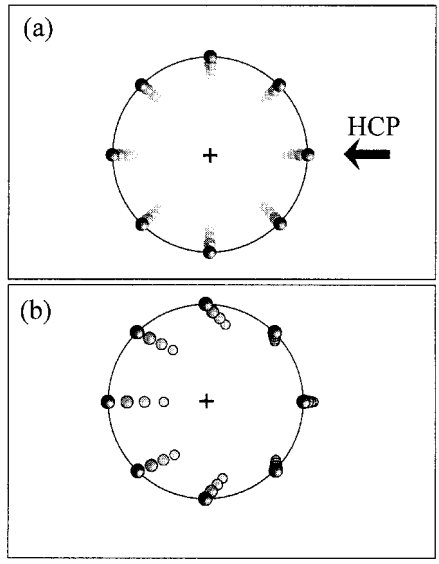

Figure 9. The probability distribution of a continuum radial wave packet may be visualized (in two dimensions) by an ensemble of classical particles moving away from the core radially. (*a*) Schematic cross-section of the ensemble at the time that the HCP is applied. (*b*) Velocities of the ensemble following the momentum kick from the HCP. The member of the ensemble on the extreme right will be kicked back into the atomic potential of the parent ion where it will form a highly localized wave packet after some time. This reasoning may be extended to three dimensions, forming a wave packet localized in all three dimensions (Jones 1996).

to excite a quasiclassical electron on a particular Kepler orbit of any eccentricity. It could allow new and exciting wave packets to be created, for example a circular wave packet embedded in an autoionization continuum will not decay through autoionization as the scattering process cannot occur.

An alternative scheme was employed by Bensky *et al.* (1998) in their efforts to unravel the recombination dynamics of an electron as it is forced back into the atomic potential. In this experiment, a radial wave packet is excited in the continuum of atomic calcium via an intermediate. The continuum wave packet behaves much like a bound wave packet but is not reflected off the atomic potential back towards the core. Recombination dynamics were then investigated by irradiating the atoms with short HCPs. With reference to figure 9, and again considering the probability distribution as an ensemble of classical particles moving out radially, the effect of the HCP is to accelerate members travelling in the direction of the field but to retard those travelling in the opposite direction. With a carefully chosen HCP field, some probability density may be returned into the grasp of the atomic potential and thus bound. Despite a lack of experimental confirmation of the existence of a space-localized wave packet formed in such a way, calculations do show that, after some time, the wave packet will rephase to form a highly localized probability distribution.

Such an excitation scheme seems particularly promising to excite highly localized coherent states similar to those described in section 3. A Schrödinger cat-like state may be created by exciting phase coherent delayed continuum wave packets which may then be forced into their desired orbits (depending on the delay between the

optical pulses) using a carefully tuned HCP. Wave packet and other studies exploiting the unique features of HCPs are rapidly increasing in number and complexity as the HCP develops into shorter and more intense pulses.

5. Non-decaying wave packets in a two-electron atom

So far, we have only considered one-electron systems, such as the first group atoms, as they are appealingly simple. In these hydrogenic systems, the electron wave packet moves around a closed-shell atomic core. However, studies of radial wave packets are certainly not restricted to one-electron atoms and have been observed to have nearly identical dynamics in a two-electron system (Strehle *et al.* 1998). Hanson and Lambropoulos (1995) suggested a control scheme in a two-electron system in which the excited wave packet would be driven into a non-decaying non-dispersing form.

Consider a typical alkaline-earth atom with a ground-state configuration $(ns)^2$. Exciting one valence electron with a short pulse to a superposition of Rydberg states leaves the remaining electron in the initial state *n*s. The excited states of this core electron represent the excited states of the ionized atom because the Rydberg electron is sufficiently weakly bound. The wave-packet system may be considered to be a one-electron atom, and the excitation of this *n*s electron may be described as an isolated core excitation (ICE) (Cooke *et al.* 1978, Wang and Cooke 1991, 1992a,b). ICE has been used in a variety of wave-packet experiments (Jones and Bucksbaum 1991, Stapelfeldt *et al.* 1991, Druten and Muller 1996, Campbell *et al.* 1998) and can be exploited to establish the electronic radial probability distribution of a wave packet (Jones 1997). In the ground state of the ion, the wave packet is bound (figure 10). However, if an ICE drives the core electron to a low-lying excited

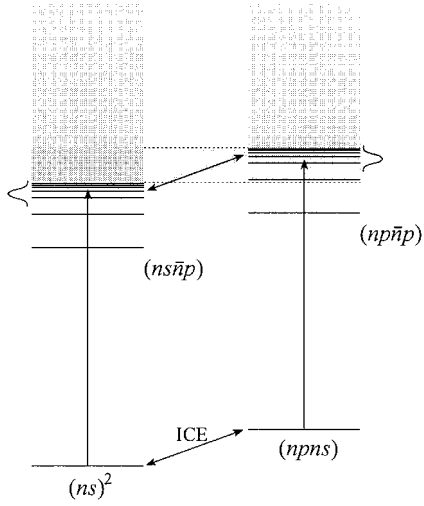

Figure 10. Excitation scheme proposed by Hanson and Lambropoulos (1995) to generate a non-dispersing wave packet in a typical two-electron system. A picosecond pulse excites a wave packet in the Rydberg series converging to the lowest ionization limit. If the remaining electron is coupled to a resonance with an intense laser field, the Rydberg states excited under the wave packet will increase in energy and become embedded in the continuum. The wave packet may now decay by autoionization (shown as a grey band).

state np, the bound wave packet will be coupled to the Rydberg series corresponding to the $np\bar{n}p$ configuration, embedded in the $ns\bar{n}p$ continuum.

A degenerate Rydberg level excited in this manner will inhibit autoionization into the continuum as a consequence of the correlation between the strongly driven core electron and the Rydberg electron, resulting in a trapping and stabilization phenomenon (Robicheaux and Hill 1996, Zobay and Alber 1996, Chen and Yeazell 1998c, Mecking and Lambropolous 1998). If the initial superposition is trapped, the superposition stays trapped for ever. If this initial condition is not fulfilled, a self-trapping mechanism, relying on Raman-like transitions with the ionization continuum, redistributes population to achieve a non-decaying superposition. In exciting a radial wave packet, this degeneracy is lifted and the trapped superposition cannot be maintained because of its time evolution. This may be compensated for by introducing an ICE field sufficiently strong for Rabi oscillations to occur between the ns and np states of the ion, such that the Rabi flopping frequency is equal to the radial orbit frequency.

Hanson and Lambropoulos used the above excitation scheme for a wave packet centred around the $\bar{n} = 50$ Rydberg state, using a Gaussian pulse with a FWHM $\tau_L = \tau_{cl}/3 = 6.3$ ps. A square pulse ICE was turned on after one orbit of the wave packet to induce the Rabi oscillation. When the wave packet makes a round trip, the core is unexcited. The ICE is switched on and population is coherently transferred to the upper Rydberg series, which lies above the ionization limit of the lower wave packet. However, decay is inhibited because the wave packet is far from the core so that there is vanishing spatial overlap between the excited core and wave packet. When the wave packet returns to the core and coincides with the Rabi flopping time, $\Omega_{ICE}^{-1} = \tau_{cl}$, the core electron will again be in its ground state and the wave packet cannot decay by autoionization. This scenario is depicted in figure 11. Decay is suppressed for several orbit periods. At longer times, the wave packet must spread in

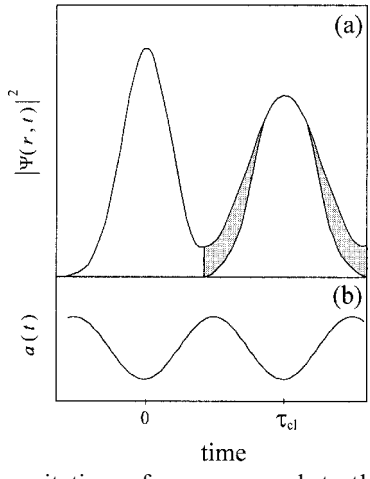

Figure 11. (*a*) After the excitation of a wave packet, the wave packet will undergo dispersion. (*b*) However, coupling the remaining core electron in a two-electron system to a state such that the electron orbit has the same frequency as the Rabi oscillation will prevent dispersion. The wings of the temporally broadened wave packet are embedded in an autoionization continuum when these parts approach the core, causing the wave packet to be shaped as shown by the grey shading in (*a*).

the atomic potential and might be expected to decay rapidly. This is, however, not the case. The wave packet is shaped into a non-spreading form and becomes analogous to a classically evolving electron. This is not like the Trojan wave packet in which the local potential is made to be harmonic. The two-electron wave packet excited here exists in an anharmonic potential.

The non-spreading wave packet may be understood by a simple physical insight. When the spread wave packet approaches the core, the low energy wing will experience a core that has not undergone the full Rabi cycle. Some population is left in the upper wave-packet states and decays. The trapping is lost as the orbit period of the spreading wings is not in phase with the Rabi period and the amplitudes overlap constructively with the continuum. The low-energy wing will experience similar decay. This means that the wave-packet is shaped into a non-dispersing form.

The reverse is also valid. An ICE switched on at τ_{cl} will cause the centre of the wave packet to decay and the wings to survive. These wings will, after the initial decay of the central part of the wave packet, be in a non-decaying form. This would form a wave packet similar to a second-order partial revival.

This non-decaying non-dispersing coupled wave packet has recently been observed by Chen and Yeazell (1998a) who excited a radial wave packet in atomic calcium. Two photons from a picosecond laser excite a wave packet with predominantly *n*d character from the $(4s)^2$ ground state. The remaining 4s electron is coupled to the 4p state of the Ca^+ ion through an ICE with a continuous-wave laser. The coupled wave packet will oscillate between the bound and autoionizing Rydberg states at the Rabi frequency. When the orbital frequency coincides with this frequency, decay is predicted to be suppressed. The wave packet is monitored at a fixed delay, which is long compared with the autoionization lifetime of a single Rydberg state, using the optical Ramsey method. Without the ICE, the wave packet is bound and reveals large-amplitude Ramsey fringes for wave packets centred around a certain $\bar{n}$ whose orbit period is an integer multiple of the time required to reach the fixed delay (figure 12). When the ICE is turned on, only the wave packet of energy $\bar{n}$ whose orbit period is synchronous to the Rabi flopping time, $\bar{n} \approx 67$, survives, as predicted theoretically. At the fixed delay for the probe pulse, figure 12 shows that there is only significant fringe amplitude around $\bar{n} = 67$, indicating strongly retarded decay with respect to the non-synchronized wave packets.

Although the shaping is a result of the non-decaying phenomenon, direct observation of the non-dispersive character of these wave packets has not yet been recorded. The time scales for such observations would be of the order of nanoseconds. The lifetime of the 4p state is only about 6 ns and so decoherent population redistribution will cause collapse of the non-decaying wave packet. Hopefully this shaping process will be observed in the near future, as it is a remarkable feature of this type of wave packet. Also, excitation of the reverse 'out-of-phase' wave packet would provide valuable insight into the process and a novel way of shaping a wave packet. The main drawback with producing such a wave packet would be that the amplitude of the wave packet is expected to be small as most is lost in the initial decay of the central part of the wave packet. Nevertheless, wave packets beyond the one-electron atom provide new wave-packet dynamics and means of manipulation.

A particularly subtle experiment employing ICE in a wave-packet atom allows the electronic radial probability distribution to be measured (Jones 1998). Here, it is

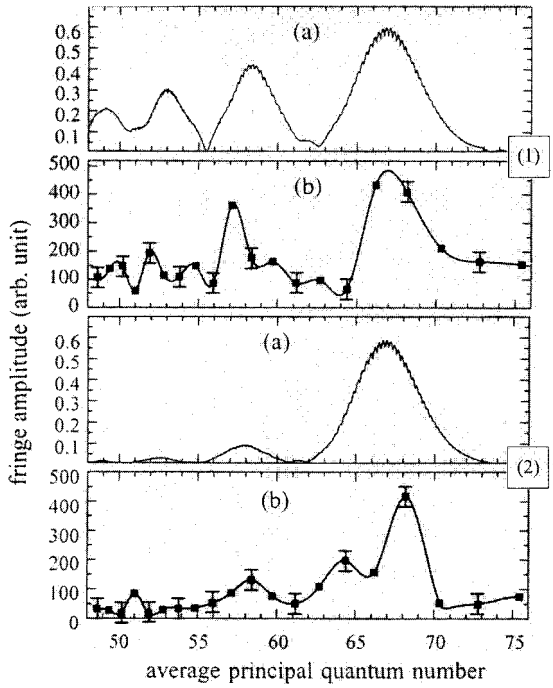

Figure 12. Amplitude of Ramsey fringes as a function of the principal quantum number n, for a wave packet (1) without a core excitation and (2) where a strong ICE is synchronized with the orbit frequency of a wave packet with average $\bar{n} = 67$. At this energy, the wave packet is in a non-decaying form: (*a*) in both cases, the calculation results; (*b*) in both cases, the corresponding experimental data. Each peak in (1) appears whenever the wave packet has undergone an integral number of orbits to reach the fixed delay time of the Ramsey probe pulse. Note that, in (2), only the synchronized case ($\bar{n} = 67$) producing a non-decaying wave packet shows a significant Ramsey fringe amplitude. (Figures 2 and 3 from Chen and Yeazell (1998c).)

not the momentum distribution that is measured, as accomplished using unipolar HCPs with the impulsive momentum retrieval method. The technique involves using a time-resolved ICE in a multielectron atom. For simplicity, however, an atom with two optical electrons is considered. Upon excitation of a Rydberg wave packet, the core electron may be excited with a time delay using a short pulse. If the optical excitation of the core electron is fast on the time scale of the wave-packet orbit, the electron will not change over the pulse duration. The spectral line shape of the ICE is critically dependent on the radial position of the wave packet (Story *et al.* 1993). Away from the core, the ICE will behave like a normal transition. The Rydberg wave packet does not interact with the core electron and the transition will have a spectral shape determined by the laser pulse. On the other hand, when the wave packet is at the core, the electrons will interact and may scatter from each other. This has the effect of broadening and shifting the core transition line shape. This shape change in the core transition line will therefore be indicative of the radial probability distribution of the wave packet. By monitoring the line shape of the ICE at different time delays and ICE frequencies, the time-dependent radial probability distribution of the wave packet may be obtained (Jones 1998).

6. The Rydberg electron in a molecule

So far we have seen that, through the interaction of external fields, the wave packet may be manipulated to inhibit or enhance decay, or to form close quantum analogues of the classical electron or even exotic wave packets. Some more fundamental interactions have recently been observed in our own group when we looked beyond the atomic systems and excited an electron wave packet in a molecule (Stavros *et al.* 1999a, b). Although simple one electron systems are excellent starting blocks to unveil fundamental electron wave-packet dynamics, molecular systems are somewhat more interesting because they present the wave packet with a non-static core. Vibrational motion occurs on a femtosecond time scale and has been investigated in its own right (Zewail 2000). Rotational motion on the other hand is several orders slower (for low quantum numbers) because the energy separations between adjacent rotational levels are only of the order of several wavenumbers. The rotational period $T_{\mathrm{Rot}} = \{2Bc[N(N+1)]^{1/2}\}^{-1}$, of a typical diatomic compound, where B is the rotational constant and N is the molecular angular momentum (excluding spin) in Hund's case (d) nomenclature, is of the order of picoseconds. For electron wave packets excited in a Rydberg series where the energy separations are comparable with those of the rotational levels, the Born–Oppenheimer approximation fails as the period of nuclear rotation is similar to the classical orbit period of the electron.

Perhaps one of the main drawbacks of looking at electron wave packets in molecules is that the density of states under the excitation pulse is far greater because numerous interleaved Rydberg series converge to different rovibrational levels of the ion. This problem may be somewhat overcome by exciting via a well-defined intermediate level. In their study, Stavros *et al.* (1999a, b) used a rotational level of the $v' = 1$ level of the A $^2\Sigma^+$ state in NO. This state is the lowest-lying Rydberg state in this molecule and consequently has a strong $\Delta v = 0$ propensity for excitation to high-lying Rydberg states. Predominantly vibrational autoionizing states are excited in Rydberg series converging to the $v^+ = 1$ limit of the ion upon irradiation with a picosecond pulse. Selectively exciting via a particular rotational state of this intermediate level allows some selectivity over the rotational states of the core of the Rydberg wave-packet system.

The optical Ramsey method was employed to induce the usual phase-dependent population of the Rydberg states. By scanning the picosecond laser over a range of central principal quantum numbers $\bar{n}$, the time of the first return of the wave packet to the core was recorded and is plotted in figure 13, together with an example of one spectrum. Clear deviations from the expected hydrogenic orbit period trend (proportional to $\bar{n}^3$) are visible at regions where the period of the electron motion is comparable with the rotational period of the ion core. This coincidence of the electronic and nuclear periods and the accompanying observed plateau suggest a strong *intra*molecular interaction in which the quasiclassical electron is coupled to the rotating dipole on the molecular ion. It should be noted that the spectrum presented in figure 13 shows a well-defined first peak, quite similar to the atomic case. The high density of states in the excitation region does, however, cause rapid dispersion of the wave packet. It should also be noted that the NO system is a rather complex diatomic compound in which the Rydberg states are strongly coupled with the autoionization continuum, dissociation continuum above the B and L valence states, and other Rydberg series.

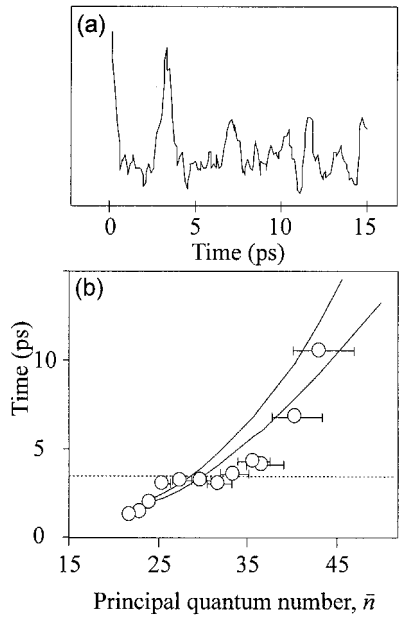

Figure 13. (*a*) A typical recurrence spectrum for a wave packet excited in NO at around $n_0 = 30$ via the $N' = 0$, $J = 1/2$ rotational level of the A state; note that the intensity is normalized on the $t = 0$ peak. (*b*) Experimental first recurrence times as a function of n_0 (○). Excitation was via the $N' = 0$, $J' = \frac{1}{2}$ level of the A state. Note that the errors in the measured times are less than the circle diameters whereas errors in n_0, arising from the uncertainty in the central wavelength of the frequency-doubled picosecond radiation (±0.1 nm), are shown in the figure: (——) calculated classical orbit periods $\tau_{cl} = 2\pi n^3$, for a wave packet composed of (*a*) *n*p(0) and (*b*) *n*p(2) states: (.....) calculated rotational period of the NO^+ core in its $N^+ = 2$ rotational state (the Born–Oppenheimer limit). Note that the experimental times are close to the classical periods except in the region of the Born–Oppenheimer limit where the rotational period of the ion core dominates. (Figure 1 from Smith *et al.* (2000).)

The graph in figure 13 shows the orbit period trend for an electron excited via the $N' = 0$ rotational level in the $v' = 1$ level of the intermediate. This electronic intermediate is the 3sσ state which has predominantly s character but also some d-character impurities. Excitation from this rovibrational level is expected to couple predominantly to $n\mathrm{p}(N^+)$ where $N^+ = 0$. Such a non-rotating core cannot couple to the electron. However, the d character is expected to play a significant role, particularly since the *n*p states are predissociating. The d character means that the states $n\mathrm{p}(N^+ + 2)$ and $n\mathrm{f}(N^+ + 2)$ are included in the superposition. The observed coupling occurs between an $N^+ = 2$ core (the rotational period of such a core is $T_{\mathrm{Rot}} = 3.5$ ps). Similar coupling may be observed for excitation via different rotational states (Smith *et al.* 2000). However, rotational periods increase rapidly with increasing rotational quantum number and so for experimental reasons cannot be observed for $N^+ > 3$.

In addition to these observations, in our investigations into the temporal behaviour at longer times, a rather surprising perturbation occurring at well-defined excitation energies has been noted. Superimposed on the peaks occurring at the classical orbit period is a much slower oscillation (figure 14) for which a proper quantitative description is still being investigated.

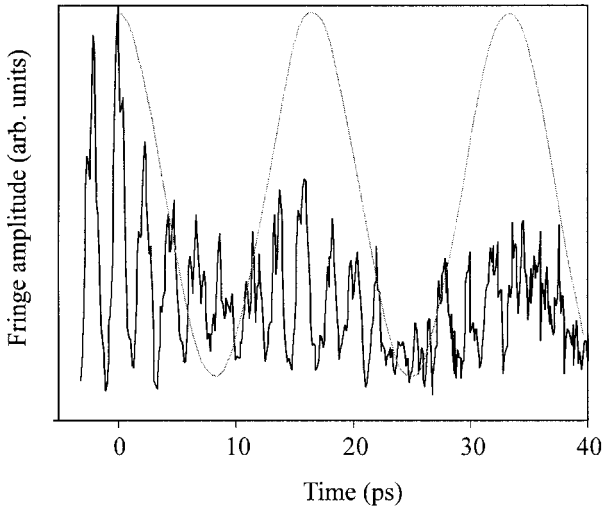

Figure 14. Amplitude of Ramsey fringes following excitation of a wave packet in NO at around $n_1 = 23$. The fast modulation has a period of 2.2 ps and represents the return of the electron wave packet to its initial composition. The slow modulation has a period of 16 ps and is most likely to be due to a coherent transfer of population between the np(1) and np(3) coupled Rydberg series.

A complementary new approach for the detection of Rydberg wave packets in a predissociating molecule is also being developed by our group. The optical Ramsey method has a major limitation in that it measures the autocorrelation function of the wave packet $\langle\psi(t)|\psi(t=0)\rangle$ which is simply the Fourier transform of the frequency domain. This is overcome in a time-dependent pump–probe type of experiment. However, as mentioned earlier, a poor signal-to-noise ratio normally makes this technique unattractive. We are proposing to excite the dissociation products in a time-resolved fashion and to distinguish between the NO^+ and N^+ ions using a time-of-flight technique. This is possible since the np states predissociate rapidly via a valence state. The atomic product may thus be ionized with a second delayed picosecond pulse (figure 15) in a Zewail-type pump-probe experiment. Additionally, the probe laser could be a femtosecond laser to gain additional sensitivity. This technique will provide valuable information about electron wave-packet behaviour in NO and could of course be applied to a range of other molecules.

7. Concluding remarks

In the last decade, and in particular in the last 5 years or so, electronic wave packets have, since their first observation (ten Wolde *et al.* 1988, Yeazell and Stroud 1988), been recognized and characterized as very important non-stationary quantum states, bordering on the classical limit of high principal quantum numbers. Coherent control schemes employed using such wave packets have proved to be of fundamental importance in our quest to understand quantum phenomena. Exotic quantum states such as the Schrödinger cat states may be excited and studied. Importantly, using a coherent control scheme, the wavefunction of a wave packet may be measured and altered to any new desired form. The implication of this

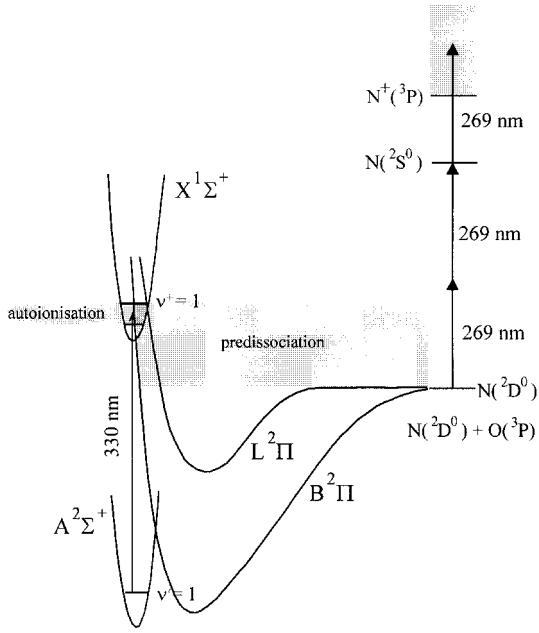

Figure 15. Excitation scheme for a proposed detection technique for predissociating molecules such as NO.

powerful tool not only is restricted to atomic, molecular or solid-state wave packets but also has recently been shown to have uses in quantum computations. Weinacht *et al.* (2000) have excited a programmable wave packet as a quantum data register. The power of quantum computing stems from the fact that a qubit, being a superposition of two states, can have more values than a classical 1/0 switch. A wave packet made of N Rydberg states may be excited in which every state in the superposition has a defined phase ϕ_n with respect to the initial state. A programmable 'search' pulse may then be used to read the data register. If the readable states are labelled by a phase $\phi_n = \pi$, then a search wave-packet phase shifted by π with respect to the original wave packet (excluding any state labelling), will enhance the Rydberg population in the labelled state as they are in phase. All the other states will be out of phase with the search wave packet and are pumped back down to the initial state. The result of the data register search may then be obtained by state-selective ionization, revealing only the labelled state.

The study of molecular Rydberg wave packets is a newly emerging field. Control of molecular electron wave packets should lead to control of dissociation, autoionization and other processes. Molecular Rydberg wave packets are much more complex than their atomic counterparts, and the characterization and measurement of their wavefunctions will be tricky as state-selective field ionization cannot resolve the various angular and rotational momentum components. Molecular systems will undoubtedly provide one of the next big challenges for both experimentalists and theoreticians.

With this review, we hope that we have provided a feel for this rapidly expanding area and the significant implications of radial electron wave packets and electron wave packets in general.

References

ALBER, G., RITSCH, H., and ZOLLER, P., 1986, *Phys. Rev.* A, **34**, 1058.

ALBER, G., and ZOLLER, P., 1991, *Phys. Rep.*, **199**, 231.

AVERBUKH, I.SH., and PERELMAN, N. F., 1989, *Phys. Lett.* A, **139**, 449.

AUSTON D. H., CHEUNG, K. P., and SMITH, P. R., 1984, *Appl Phys. Lett.*, **45**, 284.

BAUMERT, T., GROSSER, M., THALWEISER, R., and GERBER, G., 1991, *Phys. Rev. Lett.*, **67**, 3753.

BENSKY, T. J., CAMPBELL, M. B., and JONES, R. R., 1998, *Phys. Rev. Lett.*, **81**, 3112.

BERGT, M., BRIXNER, T, KIEFER, B., STREHLE, M., and GERBER, G., 1999, *J. phys. Chem.* A, **103**, 10381.

BIALYNICKI-BIRULA, I., KALINSKI, M., and EBERLY, J. H., 1994, *Phys. Rev. Lett.*, **73**, 1777.

BROERS, B., CHRISTIAN, J. F., HOGENRAAD, J. H., VAN DER ZANDE, W. J., and NOORDAM, L. D., 1993, *Phys. Rev. Lett.*, **71**, 344.

BROMAGE, J., and STROUD, C. R., Jr, 1999, *Phys. Rev. Lett.*, **83**, 4963.

BRUMER, P., and SHAPIRO, M., 1986, *Chem. Phys. Lett.*, **126**, 541; 1992, *A. Rev. phys. Chem.*, **43**, 257.

CAMPBELL, M. B., BENSKY, T. J., and JONES, R. R., 1998, *Phys. Rev.* A, **58**, 541; 1999, *Phys. Rev.* A, **59**, R4117.

CHEN, L., CHERET, M., ROUSSEL, F., and SPIESS, G., 1993, *J. Phys.* B, **26**, L437.

CHEN, X., and YEAZELL, J. A., 1997a, *Phys. Rev.* A, **55**, 3264; 1997b, *ibid.*, **56**, 2316; 1998a, *ibid.*, **57**, R2274; 1998b, *ibid.*, **58**, 1267; 1998c, *Phys. Rev. Lett.*, **81**, 5772; 1999a, *Phys. Rev.* A, **59**, 3782; 1999b, *ibid.*, **60**, 4253.

COOKE, W. E., GALLAGHER, T. F., EDELSTEIN, S. A., and HILL, R. M., 1978, *Phys. Rev. Lett.*, **40**, 178.

DE FONZO, A. P., JARWALA, M., and LUTZ, C., 1987, *Appl Phys. Lett.*, **50**, 1155.

DELANDE, D., and GAY, J. C., 1988, *Europhys. Lett.*, **5**, 303.

DRUTEN, N. J., and MULLER, H. G., 1996, *J. Phys.* B, **29**, 15.

FANO, U., 1970, *Phys. Rev.* A., **2**, 353.

FATTINGER, CH., and GRISCHKOWSKY, D., 1988, *Appl Phys. Lett.*, **53**, 1480; 1989, *Phys. Rev. Lett.*, **62**, 2961.

FIELDING, H. H., 1994, *J. Phys.* B, **27**, 5883; 1997, *J. Chem. Phys.*, **106**, 6558.

GAETA, Z. D., NOEL, M. W., and STROUD, C. R., JR, 1994, *Phys. Rev. Lett.*, **73**, 636.

GAETA, Z. D., and STROUD, C. R., JR., 1990, *Phys. Rev.* A, **42**, 6308.

GALLAGHER, T. F., 1994, *Rydberg Atoms* (Cambridge University Press).

GALLAGHER, T. F., HIMPHREY, L. M., COOKE, W. E., HILL, R. M., and EDELSTEIN, S. A., 1977, *Phys. Rev.* A, **16**, 1098.

GORDEN, R. J., and RICE, S. A., 1997, *A. Rev. phys. Chem.*, **48**, 601.

HANSON, L. G., and LAMBROPOULOS, P., 1995, *Phys. Rev. Lett.*, **74**, 5009.

HERITAGE, J. P., WEINER, A. M., and THURSTON, R. N., 1985, *Optics Lett.*, **10**, 609.

HILLEGAS, C. W., TULL, J. X., GOSWAMI, D., STRICKLAND, D., and WARREN, W.S., 1994, *Optics Lett.*, **19**, 737.

HONG, Q., RAMSWELL, J. A., STAVROS, V. G., BARNETT, C. J., and FIELDING, H. H., 1998, *Measurement Sci. Technol.*, **9**, 378.

HULET, R. G., and KLEPPNER, D., 1983, *Phys. Rev. Lett.*, **51**, 1430.

JONES, R. R., 1996, *Phys. Rev. Lett.*, **76**, 3927; 1997, *Phys. Rev.* A, **57**, 446; 1998, *ibid.*, **57**, 446.

JONES, R. R., and BUCKSBAUM, P. H., 1991, *Phys. Rev. Lett.*, **67**, 3215.

JONES, R. R., and CAMPBELL, M. B., 2000, *Phys. Rev.* A, **61**, 13 403.

JONES, R. R., and NOORDAM, L. D., 1997, *Adv. at. molec. opt. Phys.*, **38**, 1.

JONES, R. R., YOU, D., and BUCKSBAUM, P. H., 1993, *Phys. Rev. Lett.*, **70**, 1236.

JUDSON, R. S., and RABITZ, H, 1992, *Phys. Rev. Lett.*, **68**, 1500.

KAWASHIMA, H., WEFERS, M. M., and NELSON, K. A., 1995, *A. Rev. phys. Chem.*, **46**, 627.

KRAUSE, J. L., SCHAFER, K. J., BEN-NEN, M., and WILSON, K. R., 1997, *Phys. Rev. Lett.*, **79**, 4978.

LANKHUIJZEN, G. M., and NOORDAM, L. D., 1996, *Phys. Rev. Lett.*, **76**, 1784.

LYONS, B. J., SCHUMACHER, D. W., DUNCAN, D. I., JONES, R. R., and GALLAGHER, T. F., 1998, *Phys. Rev.* A, **57**, 3712.

MEACHER, D. R., MEYLER, P. E., HUGHES, I. G., and EWART, P., 1991, *J. Phys.* B, **24**, L63.

MECKING, B. S., and LAMBROPOULOS, P., 1998, *Phys. Rev.* A, **57**, 2014.
METIU, H., and ENGEL, V., 1990, *J. opt. Soc. Am.* B, **7**, 1709.
MOLANDER, W. A., STROUD, JR., C. R., and YEAZELL, J. A., 1986, *J. Phys.* B, **18**, L461.
MOROU, G., STANCAMPIANO, C. V., and BLUMENTHAL, D., 1981, *Appl Phys. Lett.*, **38**, 470.
NOEL, M. W., and STROUD, JR., C. R., 1995, *Phys. Rev. Lett.*, **75**, 1252; 1996, *Phys. Rev. Lett.*, **77**, 1913; 1997, *Optics Express*, **1**, 176.
NOORDAM, L. D., DUNCAN, D. I., and GALLAGHER, T. F., 1992, *Phys. Rev.* A, **45**, 4734.
PARKER, J., and STROUD, JR., C. R., 1986a, *Phys. Rev. Lett.*, **56**, 716; 1986b, *Physica Scripta* T, **12**, 70.
PAULI, W., 1933, *Quantentheorie*, Handbuch der Physik, vol. 24, edited by H. Geiger and K. Schee (Berlin: Springer), part 1, p. 98.
RAMAN, C., CONOVER, C. W.S., SUKENIK, C. I., and BUCKSBAUM, P. H., 1996, *Phys. Rev. Lett.*, **76**, 2436.
RAMAN, C. S., WEINACHT, T. C., and BUCKSBAUM, P. H., 1997, *Phys. Rev.* A, **55**, R3995.
RAMSWELL, J. A., and FIELDING, H. H., 1998, *J. Chem. Phys.*, **108**, 7653.
RAMSWELL, J. A., STAVROS, V. G., LEI, J., HONG, Q., and FIELDING, H. H., 1999, *Phys. Rev.* A, **59**, 2186.
RELLA, C. W., TEXIER, F., NOORDAM, L. D., and ROBICHEAUX, F., 2000, *Phys. Rev. Lett.*, **85**, 4233.
REINHOLD, C. O., and BURGDÖRFER, J., 1996, *Phys. Rev.* A, **54**, R33.
REINHOLD, C. O., MELLES, M., and BURGDRÖFER, J., 1993, *Phys. Rev. Lett.*, **70**, 4026.
ROBICHEAUX, F., and HILL III, W. T., 1996, *Phys. Rev.* A, **54**, 3276.
SCHERER, N. F., MATRO, R. J., DU, M., RUGGIERO, A. J., OMERO-ROCHIN, V., CINA, J. A., FLEMMING, G. R., and RICE, S. A., 1991, *J. chem. Phys.*, **95**, 1487.
SCHERER, N. F., RUGGIERO, A. J., DU, M., and FLEMING, G. R., 1990, *J. chem. Phys.*, **93**, 856.
SCHRÖDINGER, E., 1926, *Naturwissenschaften*, **28**, 664.
SCHUMACHER, D. W., HOGENRAAD, J. H., PINKOS, D., and BUCKSBAUM, P. H., 1995, *Phys. Rev.* A, **52**, 4719.
SCHUMACHER, D. W., LYONS, B. J., and GALLAGHER, T. F., 1997, *Phys. Rev. Lett.*, **78**, 4359.
SEATON, M. J., 1966, *Proc. phys. Soc.*, **88**, 801; 1983, *Rep. Prog. Phys.*, **46**, 167.
SHAPIRO, M., and BRUMER, P., 1986, *J. Chem. Phys.*, **84**, 4103.
SMITH, R. A. L, VERLET, J. R. R., BOLEAT, E. D., STAVROS, V. G., and FIELDING, H. H., 2000, *Discuss. Faraday Soc.*, **115**, 63.
STAPELFELDT, H., PAPAIOANNOU, D. G., NOORDAM, L. D., and GALLAGHER, T. F., 1991, *Phys. Rev. Lett.*, **67**, 3223.
STAVROS, V. G., RAMSWELL, J. A., SMITH R. A. L., VERLET, J. R. R., LEI, J., and FIELDING, H. H., 1999a, *Phys. Rev. Lett.*, **83**, 2552; 1999b, *ibid.*, **84**, 1847.
STORY, J. G., DUNCAN, D. I., and GALLAGHER, T. F., 1993, *Phys. Rev. Lett.*, **71**, 3431.
STREHLE, M., WEICHMANN, U., and GERBER, G., 1998, *Phys. Rev.* A, **58**, 450.
TANNOR, D. J., and RICE, S. A., 1985, *J. Chem. Phys.*, **83**, 5013; 1988, *Adv. chem. Phys.*, **70**, 441.
TEN WOLDE, A., NOORDAM, L. D., LAGENDIJK, A., and VAN LINDEN VAN DEN HEUVELL, H. B., 1988, *Phys. Rev. Lett.*, **61**, 2099.
TEXIER, F., and JUNGEN, CH., 1998, *Phys. Rev. Lett.*, **81**, 4329; 1999, *Phys. Rev.* A, **59**, 412.
TEXIER, F., JUNGEN, CH., and ROSS, S. C., 2000, *Discuss. Faraday Soc.*, **115**, 71.
TEXIER, F., and ROBICHEAUX, F., 2000, *Phys. Rev.* A., **61**, 43 401.
TIELKING, N. E., and JONES, R. R., 1995, *Phys. Rev.* A, **52**, 1371.
TULL, J. X., DUGAN, M. A., and WARREN, W. S., 1996, *Adv. opt. magn. Reson.*, **20**, 1.
VOGEL, K., and RISKEN, H., 1989, *Phys. Rev.* A, **40**, 2847.
UZER, T., LEE, E. A., FARRELLY, D., and BRUNELLO, A. F., 2000, *Contemp. Phys.*, **41**, 1.
WALS, J., FIELDING, H. H., CHRISTIAN, J. F., SNOEK, L. C., VAN DER ZANDE, W. J., and VAN LINDEN VAN DEN HEUVELL, H. B., 1994, *Phys. Rev. Lett.*, **72**, 3783.
WALS, J., FIELDING, H. H., and VAN LINDEN VAN DEN HEUVELL, H. B., 1995, *Physica Scripta* T, **58**, 62.
WANG, X., and COOKE, W. E., 1991, *Phys. Rev. Lett.*, **67**, 976; 1992a, *Phys. Rev.* A, **46**, 4347; 1992b, *ibid.*, **46**, R2201.

WARREN, W. S., RABITZ, H., and DAHLEH, M., 1993, *Science*, **259**, 1581.
WEFERS, M. M., and NELSON, K. A., 1993, *Optics Lett.*, **18**, 2032.
WEINACHT, T. C., AHN, J., and BUCHSBAUM, P. H., 1998a, *Phys. Rev. Lett.*, **80**, 5508; 1998b, *ibid.*, **81**, 3050; 1999, *Nature*, **397**, 233; 2000, *Science*, **287**, 463.
WEINER, A. M., 2000, *Rev. Scient. Instrum.*, **71**, 1929.
WEINER, A. M., LEAIRD, D. E., PATEL, J. S., and WULLERT, J. R., 1990, *Optics Lett.*, **15**, 326.
YEAZELL, J. A., MALLALIEU, M., and STROUD, JR., C. R., 1990, *Phys. Rev. Lett.*, **64**, 2007.
YEAZELL, J. A., and STROUD, C. R., JR., 1988, *Phys. Rev. Lett.*, **60**, 1494; 1991, *Phys. Rev.* A, **43**, 5153.
ZEWAIL, A. H., 2000, *Angew. Chem., Int. Edn.*, **39**, 2587.
ZHU, L., KLEINMAN, V., LI, X., LU, S. P., TRENTELMAN, K., and GORDON, R. J., 1995, *Science*, **270**, 77.
ZOBAY, O., and ALBER, G., 1996, *Phys. Rev.* A, **54**, 5361.